NASA Technical Memorandum 86819

Simulation Investigation of the Effect of the NASA Ames 80- by 120-Foot Wind Tunnel Exhaust Flow on Light Aircraft Operating in the Moffett Field Traffic Pattern

Barry G. Streeter

February 1986

National Aeronautics and Space Administration

NASA Technical Memorandum 86819

Simulation Investigation of the Effect of the NASA Ames 80- by 120-Foot Wind Tunnel Exhaust Flow on Light Aircraft Operating in the Moffett Field Traffic Pattern

Barry G. Streeter, Ames Research Center, Moffett Field, California

February 1986

National Aeronautics and
Space Administration

Ames Research Center
Moffett Field, California 94035

SUMMARY

A preliminary study of the exhaust flow from the NASA Ames Research Center's 80- by 120-Foot Wind Tunnel indicated that the flow might pose a hazard to low-flying light aircraft operating in the Moffett Field traffic pattern. A more extensive evaluation of the potential hazard was undertaken using a fixed-base, piloted simulation of a light twin-engine, general-aviation aircraft. The simulated aircraft was "flown" through a model of the wind tunnel exhaust flow by pilots of varying experience levels to develop a data base of aircraft and pilot reactions. This study shows that a light aircraft would be subjected to a severe disturbance which, depending upon entry condition and pilot reaction, could result in a low-altitude stall or cause damage to the aircraft tail structure.

INTRODUCTION

The 80- by 120-Foot Wind Tunnel located at the NASA Ames Research Center (ARC) at Moffett Field, CA, will soon be going into operation. The NASA Ames 80- by 120-ft wind tunnel exhausts its flow downstream of the test section out of the south end of the 40- by 80-Foot Wind Tunnel building into the atmosphere rather than containing its flow in a circuit. Figure 1 shows the 80- by 120-ft wind tunnel. A one-fiftieth-scale model of the wind tunnel was constructed and was used to determine the characteristics of the jet flow emerging from the building. Data were obtained using a two-component laser velocimeter (refs. 1 and 2) and are shown in figures 2 and 3 (ref. 3). These data show that the flow emerges from the wall of the facility at an angle of about 38° from the horizontal and about 8° east of straight south. The jet direction, velocity, and shape are all influenced by the winds blowing at the time.

An examination of the velocities in the exhaust flow of the model of the wind tunnel suggested that exhaust from the actual wind tunnel is hazardous to low-flying light aircraft which commonly operate in the Moffett Field traffic pattern. To assess the potential hazard, a fixed-base, piloted simulation was developed which included a model of the wind tunnel exhaust flow. The simulation was flown by pilots of varying experience levels to obtain representative assessments of the hazard associated with flying through the 80- by 120-ft exhaust flow in several directions and at several altitudes.

This study describes the modeling of the wind tunnel exhaust plume the simulator methods of testing aircraft response, and the pilot reactions when the aircraft is penetrating the tunnel exhaust at several altitudes and in several directions. The simulation study provided the basis for recommendations on how to minimize the potential hazard to light aircraft operating at Moffett Field when the 80- by 120-ft tunnel is operating.

SYMBOLS

ρ atmospheric density

S wing area

C_{L_o} lift coefficient at zero angle of attack

C_{D_o} drag coefficient at zero angle of attack

C_{m_o} pitching moment coefficient at zero angle of attack

C_{y_β} sideforce due to sideslip

C_{n_β} yawing moment due to sideslip

C_{n_r} yawing moment due to yaw rate

C_L nondimensionalized lift coefficient

C_D nondimensionalized drag coefficient

C_m nondimensionalized pitching moment coefficient

C_{ℓ_β} rolling moment due to sideslip

C_{ℓ_r} rolling moment due to yaw rate

C_{ℓ_p} rolling moment due to roll rate

DESCRIPTION OF THE EXHAUST FLOW

The tunnel plume was modeled in a piecewise, linear manner based on the data obtained from the two-dimensional laser velocimeter tests. At the tunnel exit, the scaled model of the wind tunnel showed the flow had a velocity of approximately 81 ft/sec (24.7 m/sec) when the wind tunnel was operating at full power (figs. 2 and 3). Because of entrainment, the flow does not dissipate immediately, but

remains relatively constant for about 400 ft (122 m) downstream of the tunnel exhaust. From this point and extending downwind, the flow velocity decreases in a linear fashion with a gradient of 0.0452 ft/sec/ft (m/sec/m). Thus, according to the simulation model, the flow diminishes to zero at 1415 ft (431 m) downwind from the tunnel exhaust. This conclusion is consistent with the results of the tests derived from the scale model (ref. 3).

The tunnel exhaust leaves the building at an angle of 38° with the ground and follows this course into the atmosphere. The exhaust plume produced by the flow spreads out at an angle of approximately 20°. The appendix describes in detail the exhaust flow model used in this simulation, which is shown in figures 4 and 5.

SIMULATION METHODOLOGY

This simulation was done at NASA ARC on a fixed-base simulator using a model of a light, twin-engine aircraft that was developed for a previous experiment. The fixed-base simulator is a general-purpose aircraft simulator that was provided for this simulation with the same equipment as the cockpit of a light, general-aviation aircraft. A terrain-board visual display was provided so that the pilot could receive visual cues. On the terrain board, the wind tunnel exhaust flow model originated (fig. 20) inside a building and exhausted out of one side of that building to more realistically model the 40- by 80-Foot Wind Tunnel building. The building also provided a visual reference for the pilots flying this simulation.

The light aircraft modeled is representative of the types of aircraft which operate in the Moffett Field traffic pattern and which are therefore likely to encounter the 80- by 120-ft tunnel exhaust flow. These light aircraft are considered to be the most vulnerable to such a disturbance. To investigate the effect of the exhaust plume on light, general-aviation aircraft, five pilots of varying experience levels were asked to fly the model through the exhaust flow while holding altitude, airspeed, and heading constant.

The simulated aircraft was modeled in the landing configuration because the light-aircraft traffic around Moffett Field that could pass through the wind tunnel exhaust will most likely be flying downwind in preparation for landing (fig. 6). The light-aircraft model contained the following representative, dimensionless derivatives for a landing configuration:

$$C_{L_o} = 0.274 \qquad C_{L} = 0.0968$$

$$C_{D_o} = 0.030 \qquad C_{D} = 0.0116$$

$$C_{m_o} = 0.044 \qquad C_{m} = -0.0097$$

$$C_{y_\beta} = -0.0079 \qquad C_{\ell_\beta} = -0.0015$$

$$C_{n_\beta} = 0.0012 \qquad C_{\ell_r} = 0.0051$$

$$C_{n_r} = -0.0019 \qquad C_{\ell_p} = -0.0079$$

The landing configuration was chosen because it has proven to be one of the most critical aircraft configurations for wind-shear disturbances because of its closeness to stall boundaries. Provisions were also made to include air traffic that frequently passes over Moffett Field en route from San Jose to the Palo Alto airport at cruise altitudes and speeds.

Pilots flew the model into the exhaust flow in calm air and then in the presence of varying levels of atmospheric turbulence. The turbulence model used was an Ames-Dryden form with scale lengths of 672.8 ft (205.1 m) in the x,y plane and RMS values ranging up to 7.5 ft/sec (2.28 m/sec). As the airplane was a point-source model, it could not include the effect of lengthwise or spanwise gradients which are present in the atmosphere.

To cover the range of possible aircraft entries into the exhaust flow, 10 different sets of initial entry conditions were developed which represent the expected headings and altitudes of aircraft flying into the exhaust. These conditions are summarized in table 1 and shown in figure 7. Entry conditions 4 through 8 represent an airplane flying across the tunnel exhaust port at different altitudes and distances. These conditions represent aircraft traversing Moffett Field from the San Jose area to the Palo Alto area. Entry conditions 9 and 10 represent aircraft in the landing configuration flying downwind in preparation for a landing at Moffett Field. Entry conditions 1 through 3 also represent aircraft flying across the tunnel exhaust port at several altitudes and distances, but the flight altitudes are lower than normal. These three conditions were included so the full effect of the tunnel exhaust on light aircraft in worst-case conditions could be studied.

Each pilot flew the model approximately 25 times into the tunnel exhaust. Strip charts were used to monitor the dynamics of the aircraft during the flights. Postflight question-and-answer sessions further documented pilot reactions to the disturbance.

THEORETICAL RESULTS

A model of a typical light aircraft was constructed to show the results of this simulation, which included or used several assumptions about characteristics common to light aircraft. Aircraft flying through turbulence or wind shear normally produce the same type of dynamic mode shapes, but with the magnitude of the dynamics governed by the wing loading. To take this into account, the model was extended by varying the wing loading throughout the range of conditions in which light aircraft typically operate.

One of the biggest hazards for light aircraft is a stall at low altitudes. Aircraft flying through the exhaust of the wind tunnel will encounter varying

amounts of horizontal and vertical wind shear which, depending upon pilot reaction, can end in a stall or in direct ground contact. The vertical component of the wind shear increases the aircraft's angle of attack; this is aggravated at low speeds by the reduced stall margins caused by airspeed fluctuations. The following theoretical analysis shows the effect of a wind shear produced by the wind tunnel on light aircraft with different levels of wing loading.

The vertical model that was used was the basic lift equation:

$$W = L = \frac{1}{2} \rho V^2 C_L S$$

or

$$\left(\frac{W}{S}\right) = \frac{1}{2} \rho V^2 C_{L_\alpha} \alpha$$

The model used standard sea-level density of 0.0023780 slugs/ft^3 (1.225 kg/m^3) and a lift-curve slope of 5.4 per radian. A maximum angle of attack of 15° was chosen as typical of many light aircraft.

An aircraft stall boundary defines the maximum vertical-gust velocity that can be safely encountered at a particular airspeed and wing loading. The incremental angle of attack produced by the vertical wind shears of the wind tunnel is shown in figure 8 for a range of true airspeeds. The figure plot was produced by a simple vector analysis of true airspeed and an incremental vertical-gust magnitude. Figure 9 shows that pilots flying light aircraft with low wing loadings do not have a large margin of safety at approach speeds. Note also that at low airspeeds, the stall margins are a strong function of the airspeed. This indicates that any decrease in airspeed will increase the possibility of stall when flying through vertical wind shears. If these two plots are combined, an indication of stall margins to the pilot is given. Figure 10 shows the stall boundaries for the model used in this analysis. As can be seen, at typical approach speeds the vertical gust intensities do not have to be extremely large to cause an aircraft to stall.

SIMULATION RESULTS

In this simulation, a light aircraft typical of the types which operate at Moffett Field was flown through the modeled exhaust plume of the ARC 80- by 120-Foot Wind Tunnel. Aircraft flying into the wind tunnel exhaust flow experience a severe wind shear, as strong as 80 ft/sec (24.3 m/sec) close to the tunnel exhaust. Depending upon the aircraft's true airspeed and the location of the entry into the exhaust flow, the time that the airplane is subjected to wind shear can vary from 2 to 4 sec up to 10 to 15 sec. Entry headings into the exhaust plume are given in table 1 and are shown in figure 7. Pilots flying the simulation were also given the opportunity to fly their own entry headings and altitudes into the exhaust plume after the initial testing was concluded.

Two representative profiles of the X-component of the wind shear encountered by the airplane in the simulation are given in figure 11. A profile will change in size while the shape will remain approximately the same according to the location of the entry into the exhaust plume. The vertical component of the shear is obtained by multiplying the X-component by the tangent of 38°.

For aircraft entry conditions 1-6 as shown in figure 7, the aircraft penetrated into the side of the exhaust flow. For three of these conditions, the aircraft penetrated at an altitude where the centerline of the flow lies; here the effects of velocities are most severe. For the remaining three conditions, the aircraft entered the flow where the effect of the shear was reduced. Any aircraft flying into the wind tunnel exhaust flow from the side will experience approximately the same response. The magnitude of the response (slope of the jet boundaries) is a function of the magnitude of the wind shear and of how fast the exhaust plume is encountered. An aircraft flying across the flow will weathercock into the flow, which will excite the dutch-roll mode and, because of the vertical component of the exhaust flow, the aircraft will also climb.

Entry conditions 1 and 2 represented maximum-disturbance situations with disturbance greater than will be encountered by aircraft operating at normal pattern altitude. Although these conditions are unlikely to occur, they served the purpose of examining both the aircraft and pilot reactions to a very severe upset. Entry conditions 3 through 6 represented situations that are likely to be encountered when light planes transit across Moffett Field.

Entry condition 1, which represented an airplane operating well below the traffic pattern altitude, provided the closest flightpath across the tunnel exhaust port. A light aircraft flying into the exhaust flow in or near this flight condition will experience sideslip excursions of approximately 11° and roll angles of 8°. However, this model may not represent the actual behavior because the model did not include such effects as that of airspeed gradients over a finite wing-span. Aircraft weathercock stability induced an airspeed increase of about 8 knots and caused the aircraft to pitch nose-down about 10° as the shear was encountered. As the aircraft was flown out of the flow, the airspeed recovered to nominal and the aircraft pitched up 10°. The time histories of these dynamics are given in figures 12 and 13. The model experienced accelerations of 0.5 g both laterally and in the normal direction. The roll, pitch, and yaw rates of the model in this simulation all exceeded 20°/sec and in some cases exceeded 25°/sec. At this entry point into the flow, with the airspeed of the model at 80 knots, the wind-shear encounter lasted for 2 to 3 sec. For this entry condition, the possibility of stalling the aircraft is not the primary worry of the pilot because the airplane will experience a violent lateral shear which will yaw the plane in the direction of the flow.

Aircraft which penetrated the exhaust flow in entry condition 2 experienced the same dynamics as documented in test condition 1, but the magnitude was reduced substantially because the velocity of the tunnel exhaust flow is not as great.

An aircraft flying into the wind tunnel exhaust flow at or near test condition 3 will encounter a shear velocity of approximately 38 ft/sec

(11.6 m/sec). Although the aircraft will not be affected as strongly as was the case in entry condition 1, the response could be detrimental. Light aircraft flying into this condition can expect sideslip and roll excursions as large as 10°. The aircraft will pitch down as much as 10° as the jet is encountered and then will recover to nominal as the flow is exited. Time histories of the aircraft dynamics are shown in figures 14 and 15.

The simulation studies show that the combination of altitude (940 ft) (286.5 m), the range from the tunnel exhaust (1200 ft) (365.8 m), and duration of the disturbance define a boundary which light aircraft should avoid while the 80- by 120-ft tunnel is operating at maximum speed. The remaining entry conditions that were chosen for lateral excursions (Nos. 2, 4, 5, 6) through the jet area did not disturb the aircraft substantially. Simulated, moderate, atmospheric turbulence could upset the aircraft more than did the remaining entry conditions as atmospheric turbulence tended to wash out the effect of the wind tunnel flow in all cases.

Pilots flying the simulated aircraft through the exhaust flow in the previously described flight conditions commented that when the exhaust flow was encountered, their initial reaction was to try to regain the initial attitude by working with the pedals and the wheel. However, they found that the disturbances were usually gone before they could fully respond to them. Pilots reported that if they were using the controls when the exhaust flow was exited, the control-surface deflections usually caused greater disturbance in the aircraft. Pilots commented that the best way to control an aircraft encountering the wind tunnel flow is not to use the control surfaces, but just to "ride it out."

An aircraft flying through the wind tunnel exhaust against the flow is represented by entry condition 9 and in the same direction as the flow by entry condition 10. Test condition 9 represents a light airplane encountering a combination of headwind and an upward vertical gust. The simuation model flying at 90 knots at 1000 ft (304.8 m) altitude typically experienced an airspeed increase of approximately 20 knots when it was subjected to entry condition 9 (see figs. 16 and 17). This increase in airspeed developed over approximately 3 sec, corresponding to a strengthening of the exhaust flow that was encountered. As the airplane exited the tunnel exhaust flow, the airspeed recovered back to 90 knots, and if the pilot was not careful, the airspeed would drop to about 80 knots. These airspeed fluctuations were accompanied by altitude variations as well. When entering the exhaust flow at an initial entry condition of 1000 ft (304.8 m), the model experienced an increase in altitude of approximately 130 ft (39.6 m) with a maximum rate of about 25 ft/sec (7.6 m/sec). The increase in altitude lagged behind the increase in exhaust flow velocities. The maximum exhaust-flow velocity was encountered 3 sec after entry, but the entire increase in altitude took approximately 10 sec to be reached. A light aircraft entering the exhaust flow in this test condition at 1000 ft (304.8 m) will react to the exhaust flow, but will not be in danger of stalling or losing altitude.

Entry condition 9 was repeated at an entry altitude of 500 ft (152.4 m) so the pilot could experience flight in other portions of the exhaust envelope. At 500 ft (152.4 m), the maximum shear velocity encountered was approximately 69 ft/sec

(21 m/sec). The wind shear was encountered very abruptly: an aircraft flying through it at 100 knots would transit the exhaust flow in less than 2 sec. Climb rates of 50 ft/sec for a period of 1 sec were accompanied by an airspeed increase of 22 knots and an 18° nose-up pitch. At an altitude of 500 ft (152.4 m), the magnitude of the response of the airplane was greater than the response from an initial altitude of 1000 ft (304.8 m), but the timespan was so small that the pilot might not have attempted to respond. As expected the airplane did not stall or lose altitude under this entry condition.

Entry condition 10 represents a common Moffett Field approach pattern that takes light aircraft downwind over the 80- by 120-ft tunnel exhaust flow. A light aircraft entering the exhaust flow from this heading will experience loss of both airspeed and altitude. The aircraft will pitch down violently upon entering the exhaust flow. Figures 18 and 19 give the time histories of this entry condition. Pilots flying this simulation were told that their task was to hold altitude, heading, and airspeed constant. When pilots flew this test condition, their initial reaction was to pull back on the stick to compensate for the pitch-down motion of the aircraft. This reaction was detrimental because when the pilot pulled back on the stick, the angle of attack increased to levels approaching a stall. When this pilot reaction was coupled with the airspeed decrease caused by the horizontal shear, the result was a complete stall. Recovery from this stall could not be assured because the airplane was close to the ground (1000 ft (304.8 m) in entry condition 10) when it entered the wind tunnel exhaust flow. As aircraft-entry altitudes decreased, this stalling was much more frequent. At entry altitudes above 1000 ft (304.8 m), the stalling was so dramatically decreased that danger to a light twin-engine aircraft was eliminated. As discussed before, any atmospheric turbulence will tend to mask the pitch-down and stalling effects.

As these simulation results were obtained from a model of a light, twin-engine aircraft, it should be noted that the wing loading of this aircraft was 21 lb/ft^2 (102.5 kg/m^2) compared to a value of 10 lb/ft^2 (48.8 kg/m^2) for a typical, light, single-engine trainer. As shown in figures 8 to 10, airplanes with lighter wing-loadings are more susceptible to a given wind shear than are heavier airplanes such as a light, twin-engine airplane. Much of the air traffic around Moffett Field is composed of smaller aircraft such as light trainers with lighter wing-loadings. These light trainers typically have wing loadings as low as 10 lb/ft^2 (48.8 kg/m^2). At an altitude of 1000 ft (304.8 m), passage through the exhaust flow may cause some concern for the flight safety of a light, twin-engine aircraft, but may actually be hazardous for lighter aircraft.

The light, twin-engine plane which was modeled has a maximum wing loading of 21 lb/ft^2 (102.5 kg/m^2) at a gross weight of 4100 lb (1860 kg). To check the validity of this simulation, the stall characteristics of the model were checked against the data shown in figures 8 to 10. For entry condition 10, the airplane entered the exhaust from an altitude of 1000 ft (304.8 m). At this altitude the vector components of the exhaust flow are 30 ft/sec (9.1 m/sec) shear horizontally and 23 ft/sec (7 m/sec) vertically. The airspeed at entry to the exhaust flow is 90 knots. A comparison of the light, twin-engine model against the composite model

used for figure 10 shows that the entry condition does result in a stall. This shows the simulation to be generally correct in the longitudinal direction.

CONCLUSIONS AND RECOMMENDATIONS

In this simulation, the flight of a light, general-aviation, twin-engine aircraft was examined via a model of the exhaust plume from the NASA Ames 80- by 120-Foot Wind Tunnel to determine whether the exhaust plume poses a safety hazard. Tests were performed at 10 sets of initial entry conditions and other pilot-selected entry conditions. The simulation showed that light aircraft flying through the wind tunnel exhaust flow below 1000 ft (304.8 m) would be subjected to conditions detrimental to the safe operation of the aircraft. These conditions could result in the aircraft entering a low-altitude stall. Test condition 10, which is representative of an aircraft flying downwind in preparation for a landing at Moffett Field, is the most troublesome situation for a light aircraft flying close to the wind tunnel exhaust flow. This flightpath pattern probably is also the most common flightpath taken by pilots flying by the wind tunnel. From estimates of the influence of wing loading, the effect of the wind tunnel exhaust can be generalized to aircraft with different wing loadings; these generalizations were validated for the specific aircraft simulated.

RECOMMENDATIONS

1. The results of this simulation study should be verified with a controlled flight test of a light, general-aviation aircraft flown by a NASA Ames research pilot. Smoke generators should be used to mark the boundaries of the wind tunnel wake.

2. The results of this report, when validated by subsequent flight tests, should be incorporated into a Notice to Airmen (NOTAM) describing the hazard of transiting the 80- by 120-ft tunnel exhaust.

3. NASA Ames should work with the Navy to develop a Moffett Field traffic pattern which will routinely keep light aircraft away from the 80- by 120-ft tunnel exhaust wake. A communication link between the 80- by 120-ft tunnel operations room and the Moffett Field control tower may be required so the tower operators can issue safety advisories to local traffic as a standard part of the takeoff and landing clearance.

NOTE: Where metric units are not given (in the figures), the following formula may used to convert the customary units to metric units:

Multiply feet by 0.3048 to get equivalent number of meters.

REFERENCES

1. Reinath, M. S.; Orloff, K. L.; and Snyder, P.K.: A Laser Velocimeter System for the Ames 40- x 80-Foot and 80- x 120-Foot Wind Tunnels. AIAA Paper 84-0414, Jan. 1984.

2. Reinath, Michael S.; Orloff, Kenneth L.; and Snyder, Philip K.: A Laser Velocimeter System for Large Scale Aerodynamic Testing NASA TM-84393, Jan. 1983.

3. Rossow, V. J.; Schmidt, G. I; Reinath, M. S.; VanAken, J. M.; and Parrish, C. L.: Experimental Study of Flow Deflectors Designed to Alleviate Ground Winds Induced by Exhaust of 80- by 120-Foot Wind Tunnel. NASA TM-88195, Jan. 1986.

APPENDIX

DESCRIPTION OF THE 80- BY 120-FOOT WIND TUNNEL EXHAUST FLOW

This appendix describes the modeling of the exhaust flow of the 80- by 120-ft open-throat wind tunnel at NASA ARC. This model was used in a digital computer simulation of light, general-aviation aircraft flying through the exhaust of the wind tunnel to determine whether flight safety is compromised because of the exhaust flow.

By definition, the virtual origin "0" of the exhaust flow is located at the intersection of the ground and the 38° centerline of the jet (fig. 20) at a point 125 ft (38 m) "behind" the tunnel exhaust port. The exhaust flow is represented vectorally in the X and Z directions. The flow component in the Y direction is assumed to be zero. The 38° centerline extending from the virtual origin is the reference line for all wind calculations.

X-DIRECTION WINDS

The winds in the X-direction are modeled as piecewise-continuous functions of X,Y,Z relative to the centerline. Figure 21 shows that along the centerline and on either side of the centerline (a distance of 83 ft (25 m)) in the Y-direction), the flow in the X-direction is to be a constant 64 ft/sec (19.5 m/sec) up to a distance of 425 ft (129 m) along the X-direction from the virtual origin. From 425 ft to 1841 ft (561.1 m) (in the X-direction), the velocity in the X-direction is modeled as a linear relationship with a slope of -0.0452 ft/sec/ft. Thus, at a distance of 1000 ft (304.8 m), the vector component of the jet is 64 + (1000 - 425) (-0.0452) = 38 ft/sec along the centerline and for 83 ft (25.3 m) on either side of the centerline. To extend the X-component of the jet to the boundary of the flow, the boundary is defined to spread out from the exhaust opening at an angle of 22° to the left of the centerline and 15° to the right. An A (1-cos y) relationship is then applied to describe the character of the jet flow from 83 ft (25.3 m) to the jet boundary, with the amplitude A defined by the V_x = constant boundary condition. What has been modeled up to this point is the jet flow along the 38° centerline extending out to the boundaries in a plane. Extension of the jet flow in the X-direction to the vertical boundaries of the flow is shown in figures 22 and 23. The top boundary of the jet will have its origin at zero and extend out at 50° in the vertical plane. This boundary will extend in the ±Y directions to the side boundaries defined previously. The lower boundary of the jet flow extends up at an angle of 38° from the ground but, unlike the centerline, it is offset along the X-axis 595 ft (181.3 m). Thus, the defining equation of the lower boundary is Z = X tan (38°) - 465 ft. The flow component of the jet in the X-direction will be modeled as an A (1-cos Z) before, with the amplitude

A (1- cos Z) relationship as before, with the amplitude A determined by the velocity V_x at the 38° centerline.

Z-DIRECTION WINDS

The magnitude of the jet flow in the Z-direction is determined solely by the magnitude of the jet in the X-direction and the constraint that the resulting total-velocity vector must lie at a 38° incline from the X-axis. For example, at a distance of 400 ft (121.9 m) from the virtual origin along the X-axis, the component of the jet velocity is 64 ft/sec. Thus the Z-component must be

$$V_z = V_x \tan (38°)$$

$$V_z = 64 \tan (38°) = 50 \text{ ft/sec}$$

Therefore, the magnitude of the total velocity vector at this location is determined by V_t (642 + 502) = 81.2 ft/sec.

This algorithm was programmed in FORTRAN and inserted into the generic-wind-model subroutine as an additional subroutine. The FORTRAN code is given in figure 24.

TABLE 1.- TABULATION OF AIRCRAFT ENTRY CONDITIONS

Condition	Distance from exhaust port, ft	Altitude, ft	Airspeed, knots
1	600	470	90
2	600	625	90
3	1200	940	90
4	1200	1250	90
5	1800	1400	90
6	1800	1875	90
7	990	800	100
8	990	1200	100
9	Flying down centerline	1000	120
10	Flying down centerline	1000	90

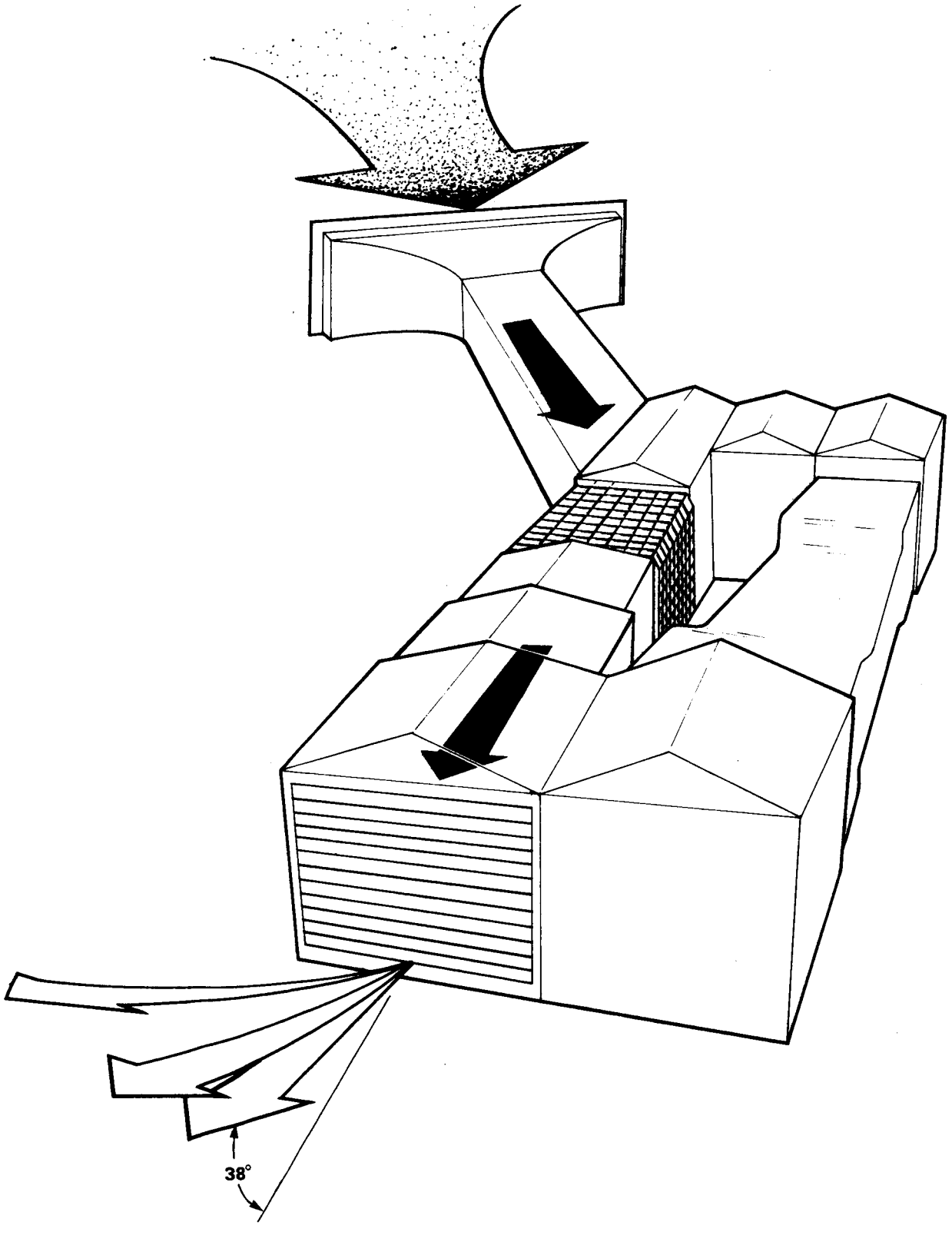

Figure 1.- Wind tunnel in 80- by 120-ft mode.

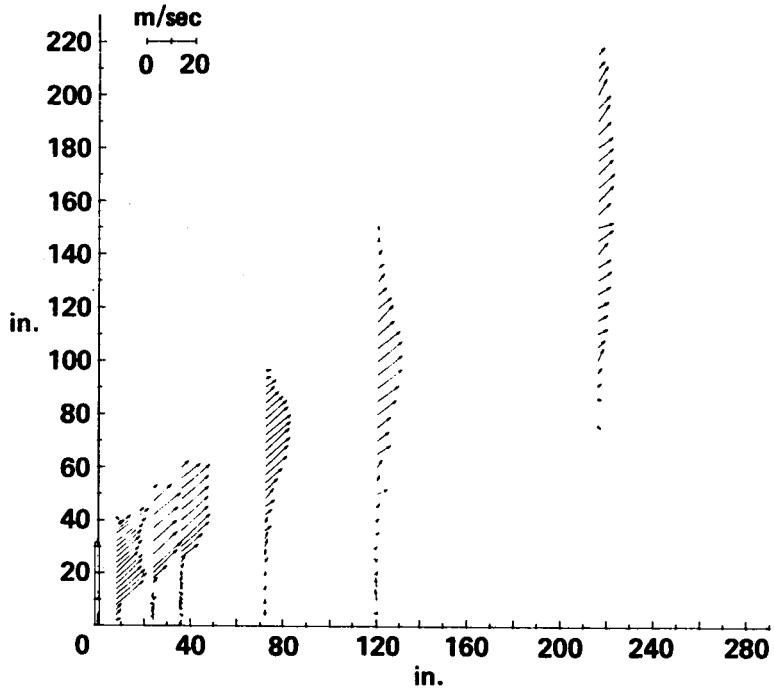

Figure 2.- Side view of raw data from velocimeter.

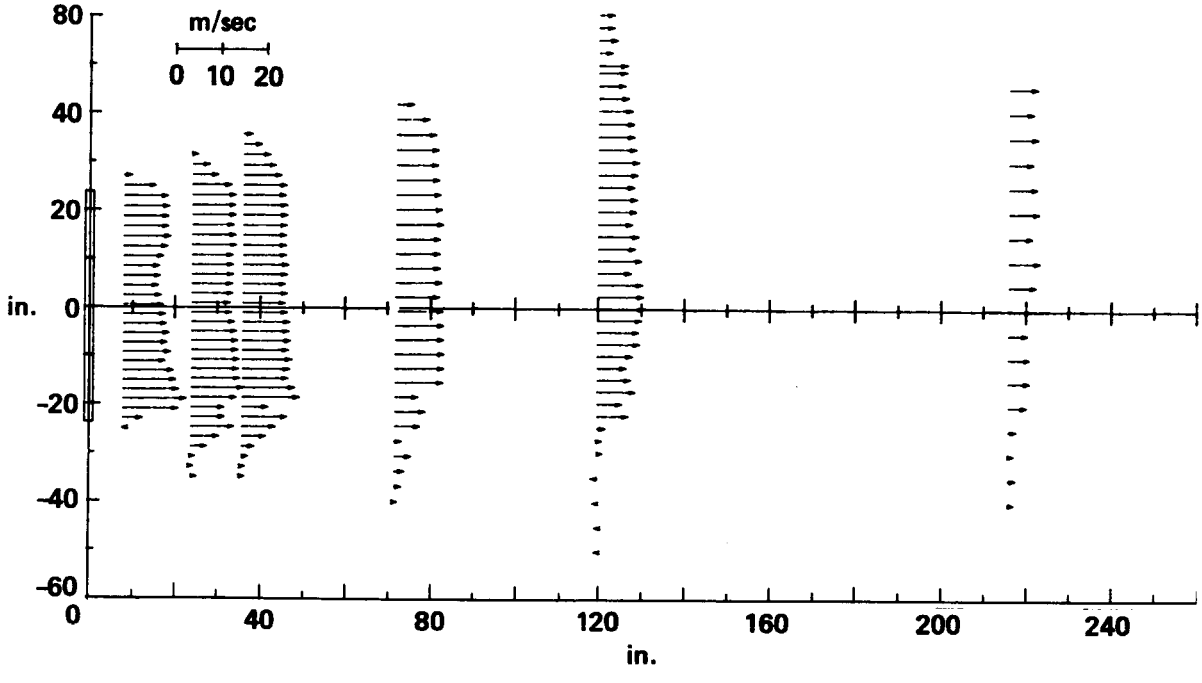

Figure 3.- Planview of raw data from velocimeter.

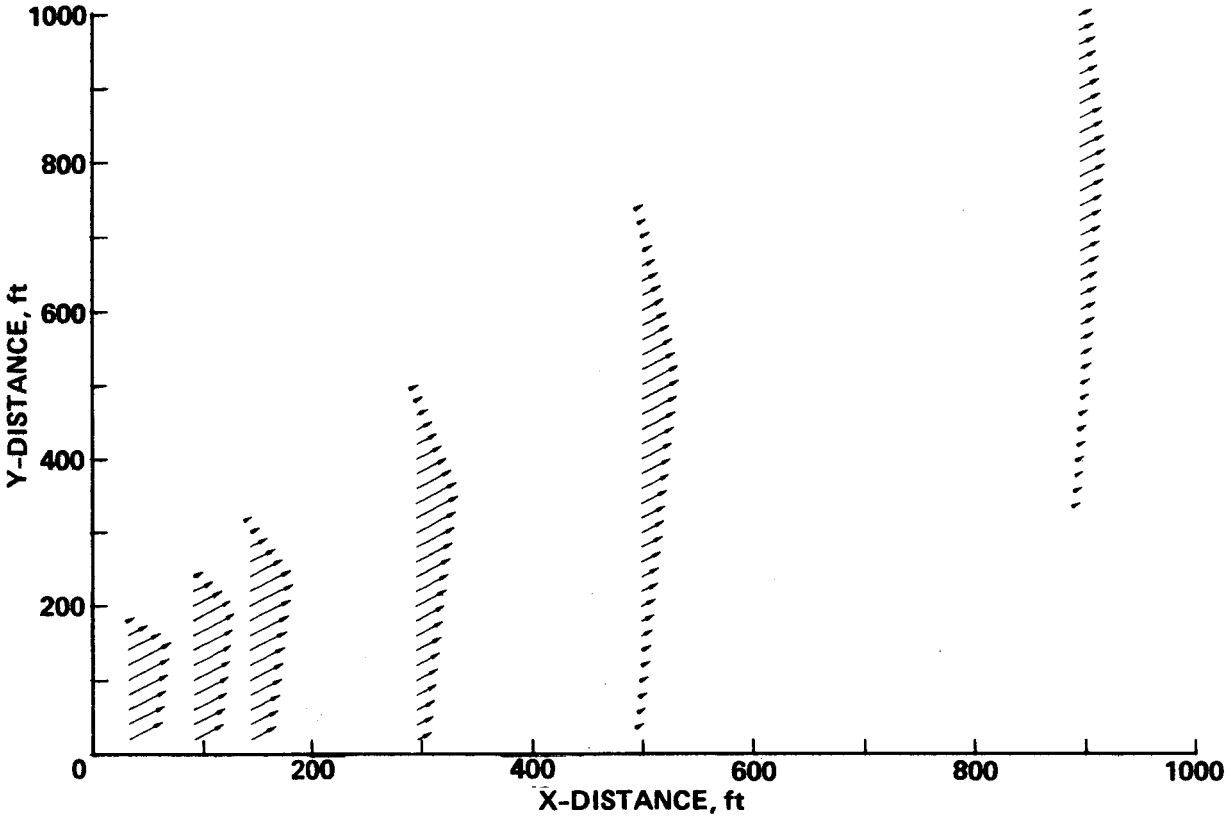

Figure 4.- Side view of wind tunnel flow model.

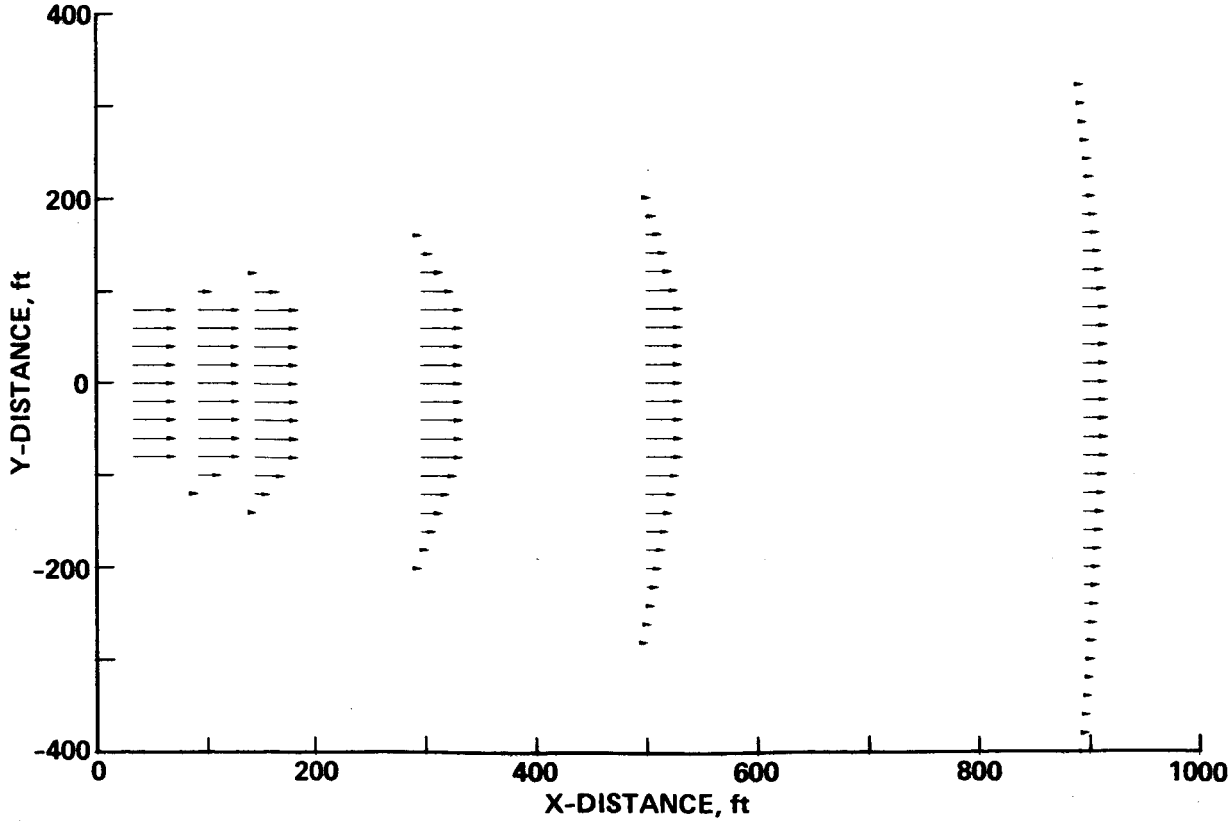

Figure 5.- Planview of wind tunnel flow model.

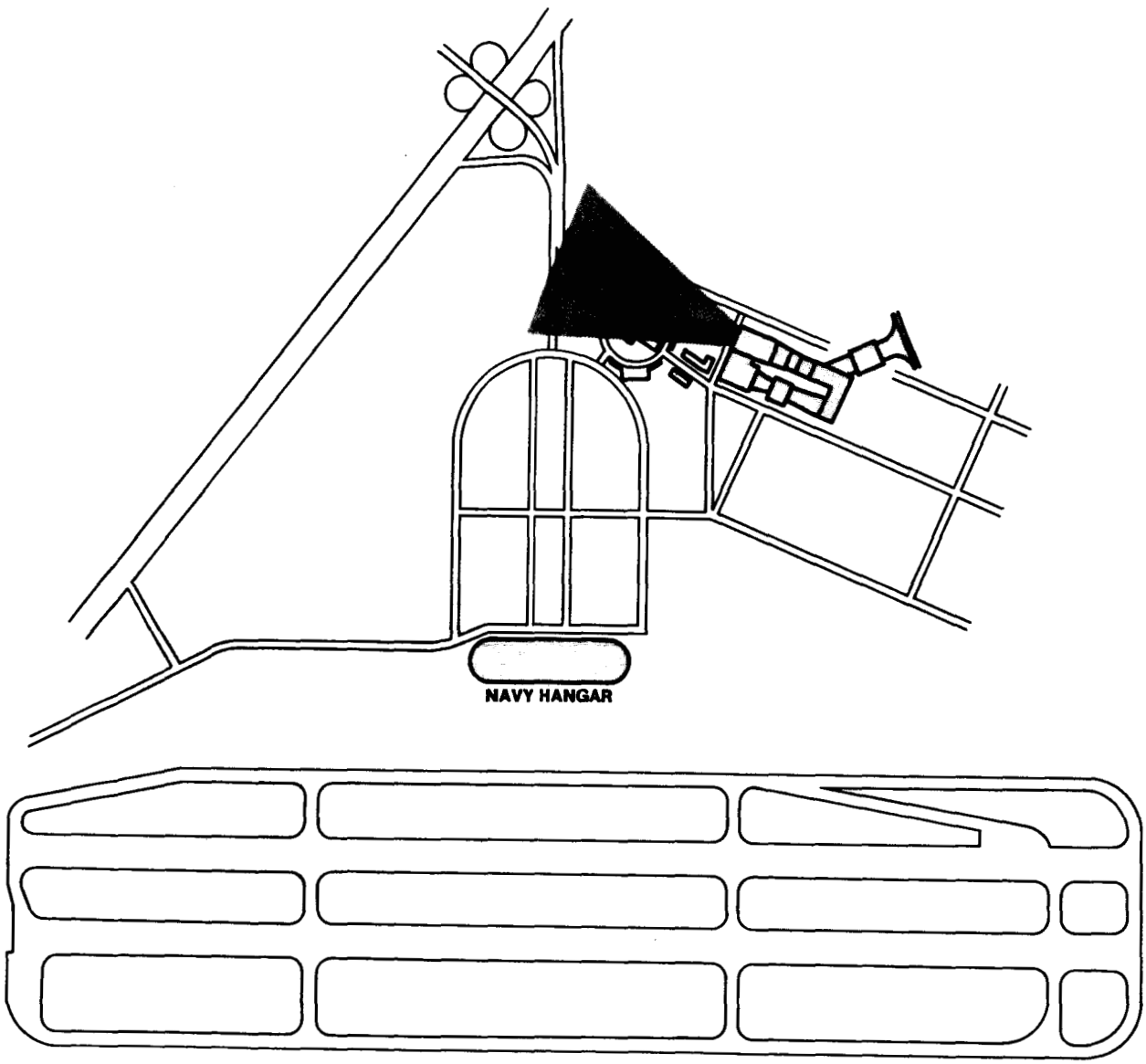

Figure 6.- Relation of wind tunnel exhaust plume to Moffett Field runways.

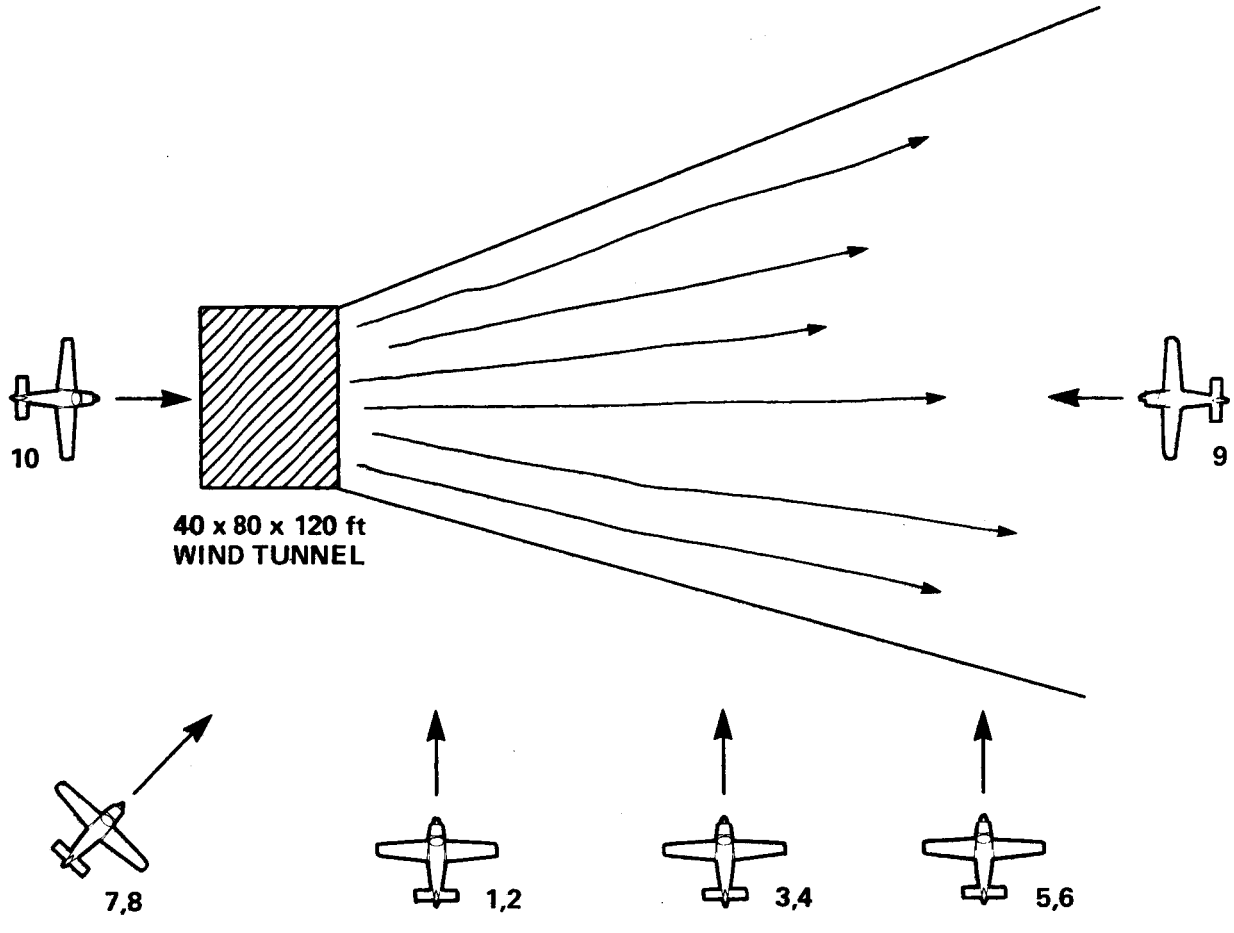

Figure 7.- Planview of aircraft test entry conditions.

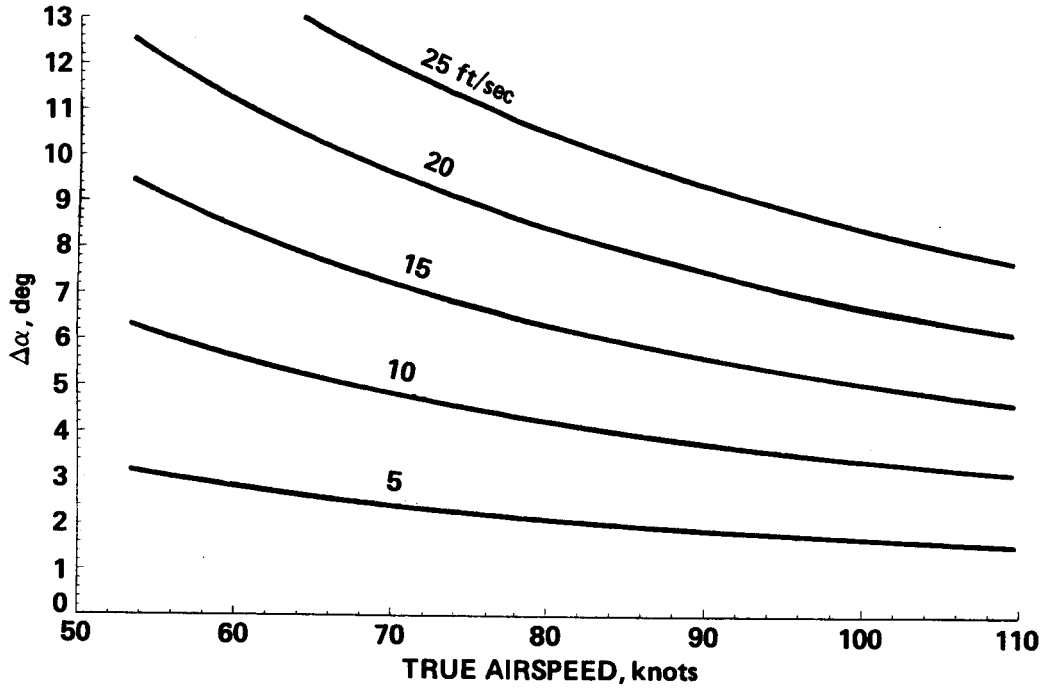

Figure 8.- Incremental angle of attack produced as a function of vertical gust velocity.

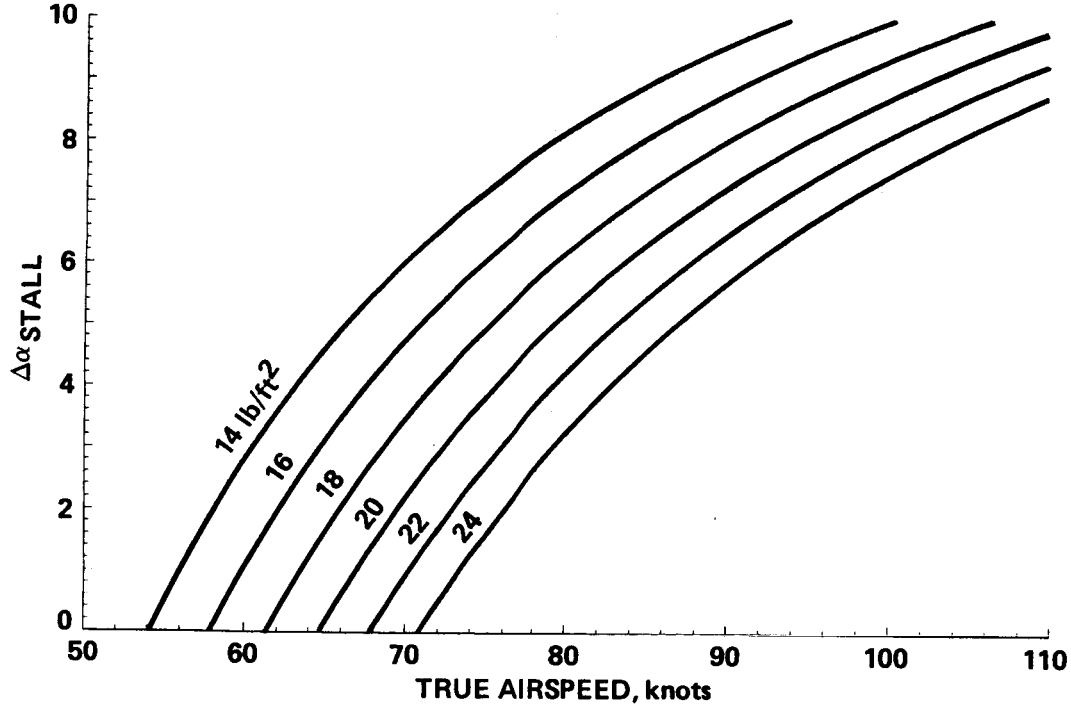

Figure 9.- Stall margins for typical light planes as a function of wing loading.

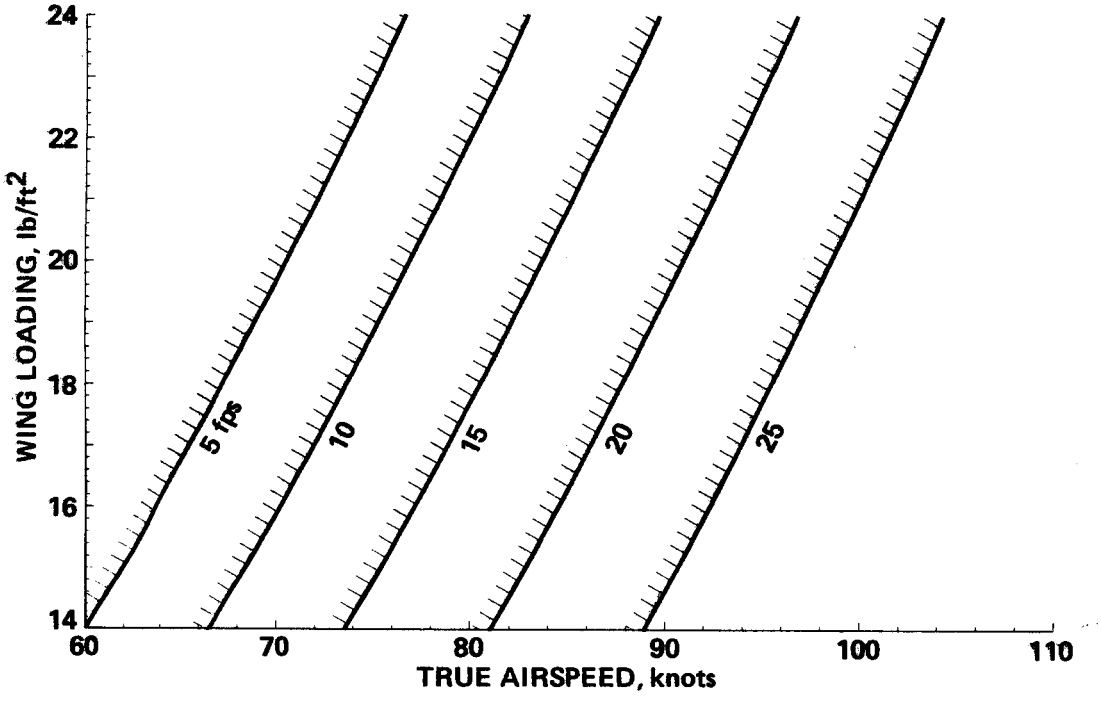

Figure 10.- Stall boundaries for typical light aircraft for varying values of wing loading.

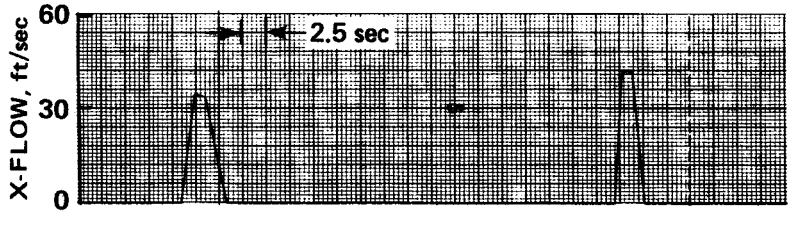

Figure 11.- Time history of exhaust profile.

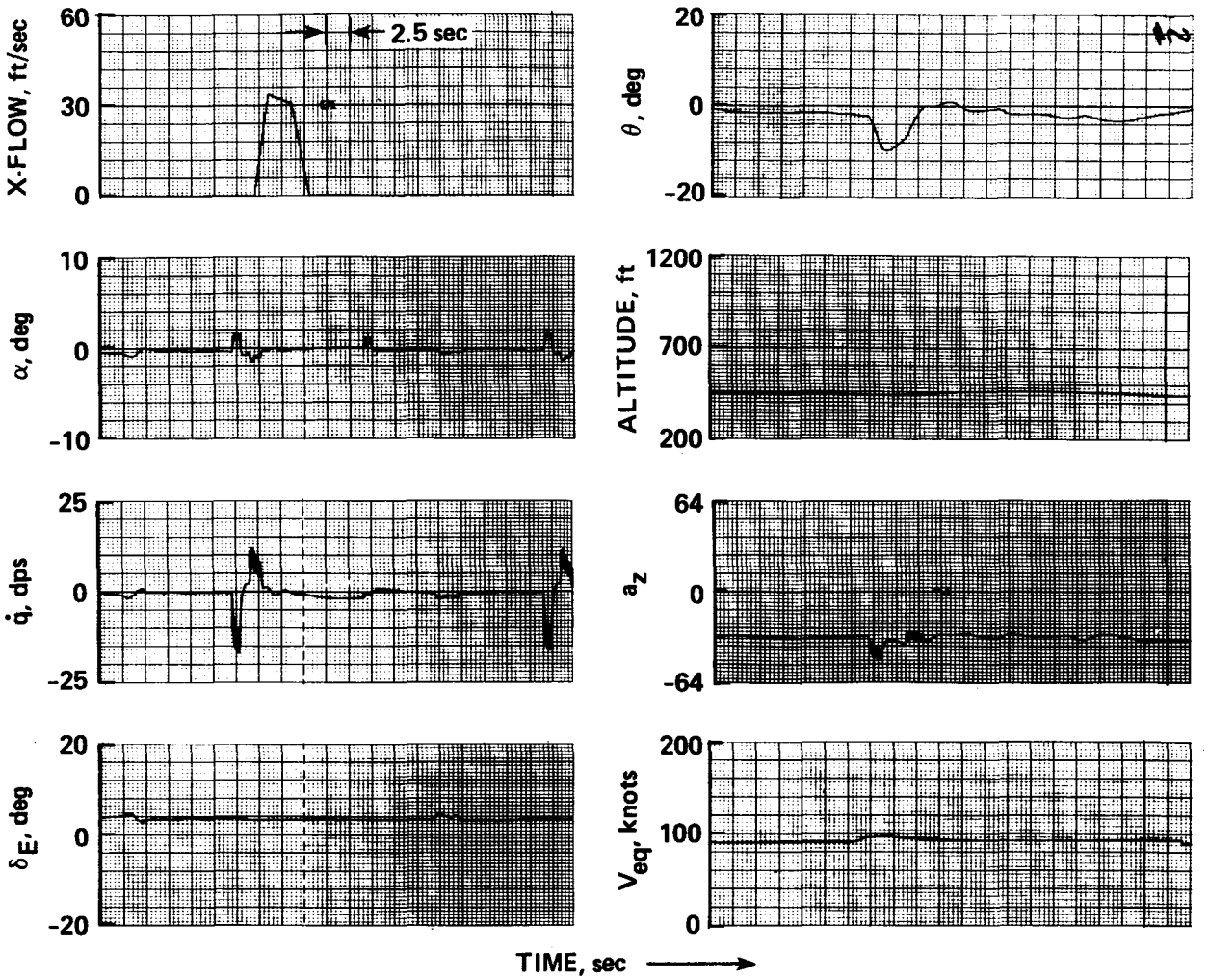

Figure 12.- Time history of entry condition 1--longitudinal traces.

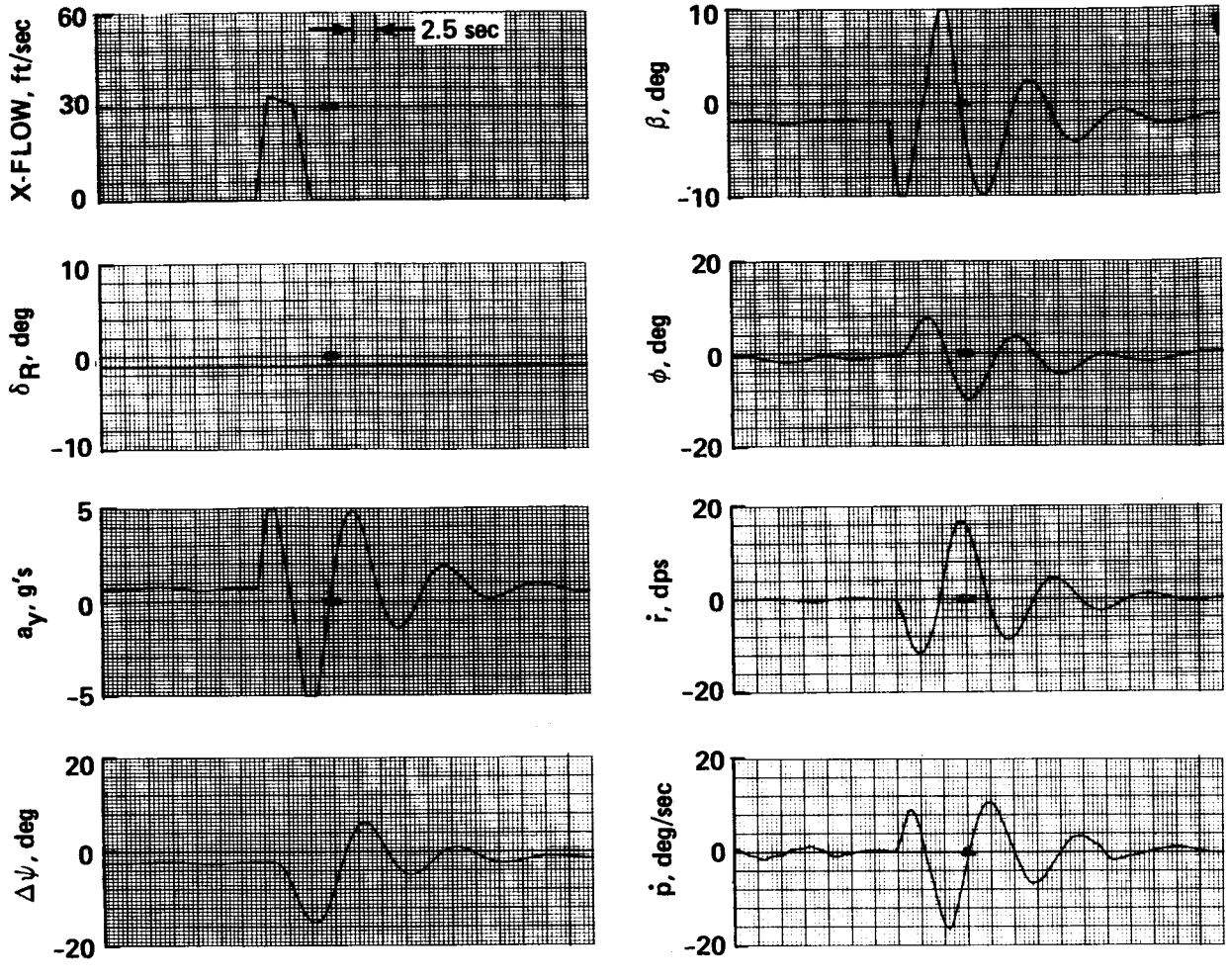

Figure 13.- Time history of entry condition 1--lateral traces.

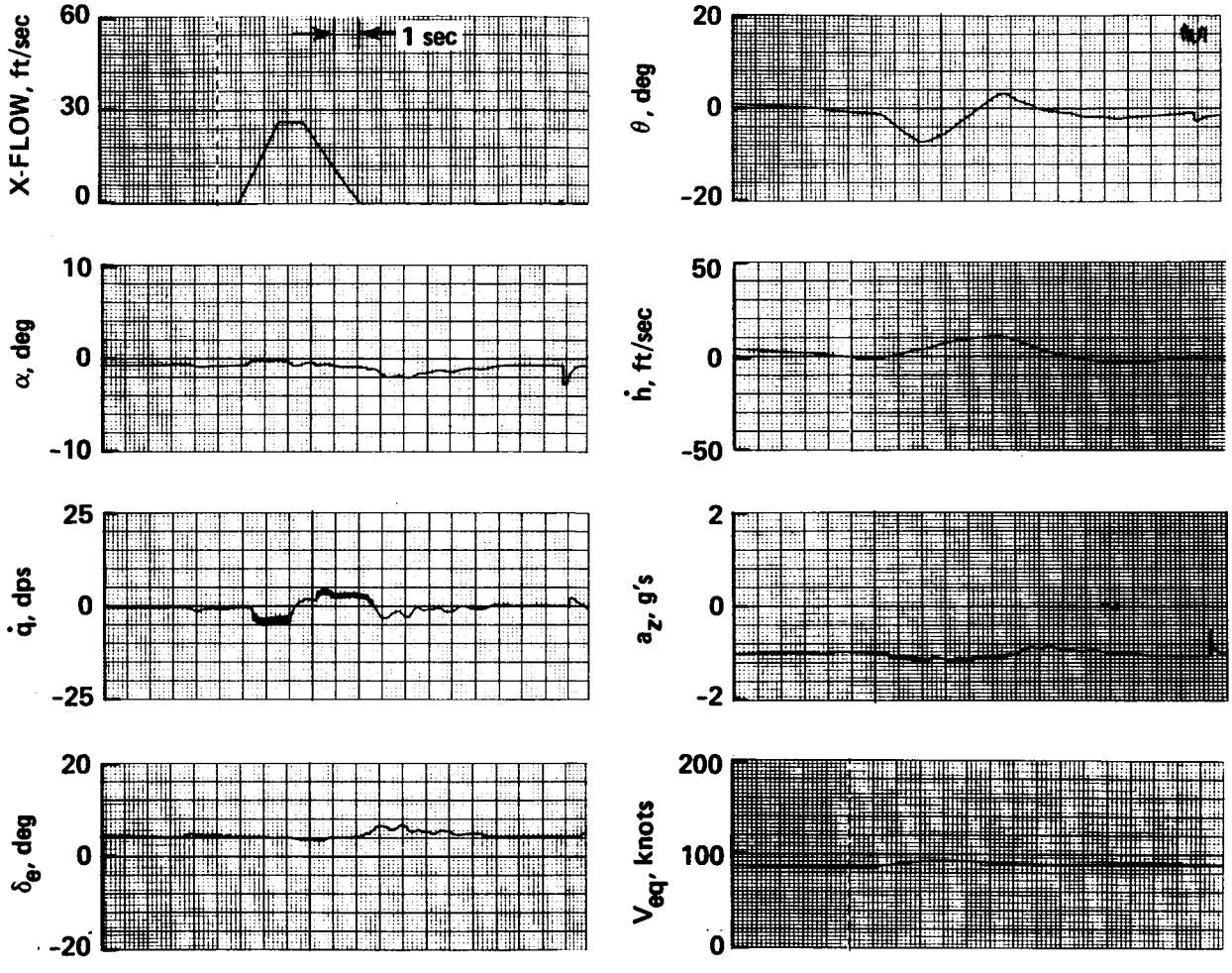

Figure 14.- Time history of entry condition 3--longitudinal traces.

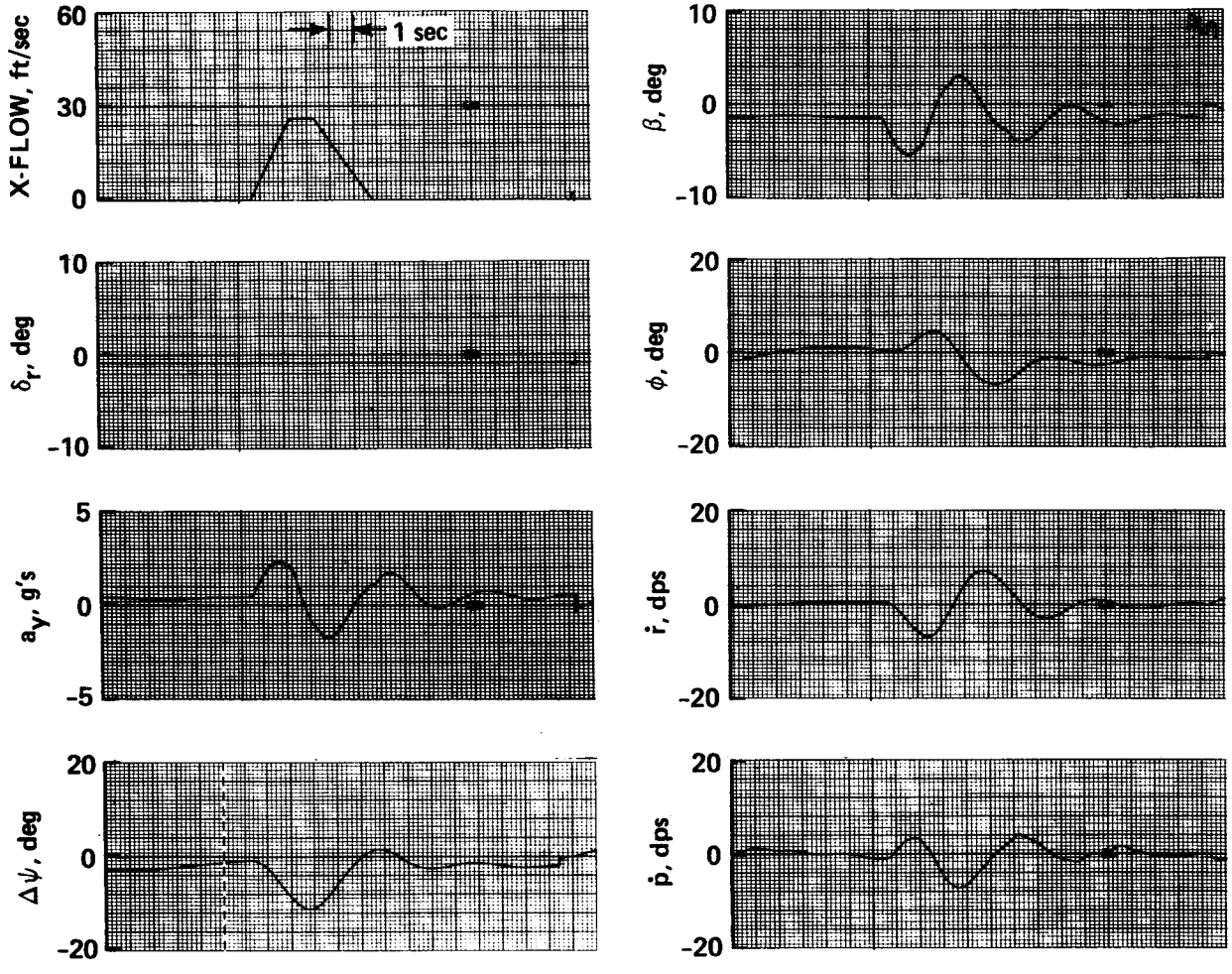

Figure 15.- Time history of entry condition 3--lateral traces.

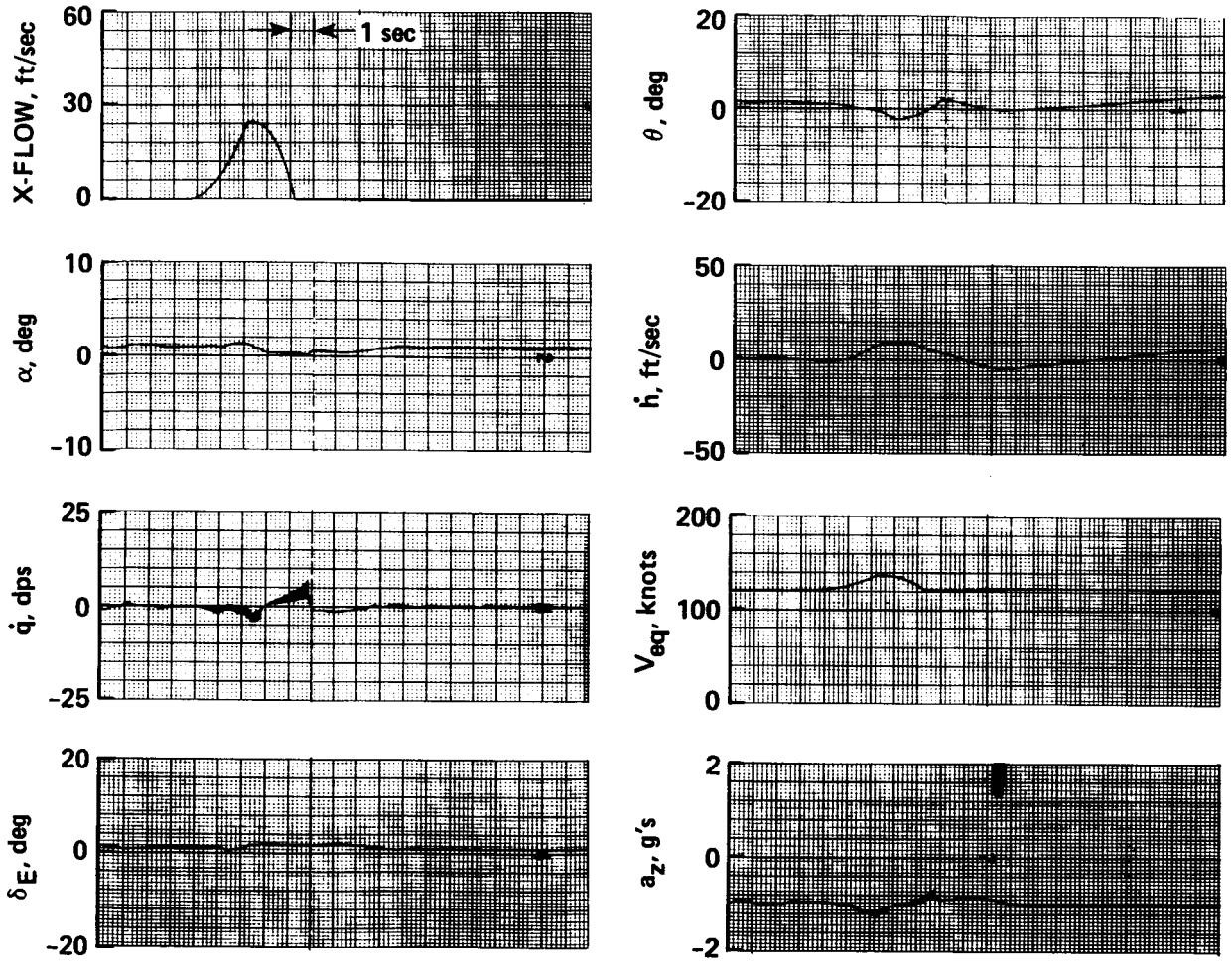

Figure 16.- Time history of entry condition 9--longitudinal traces.

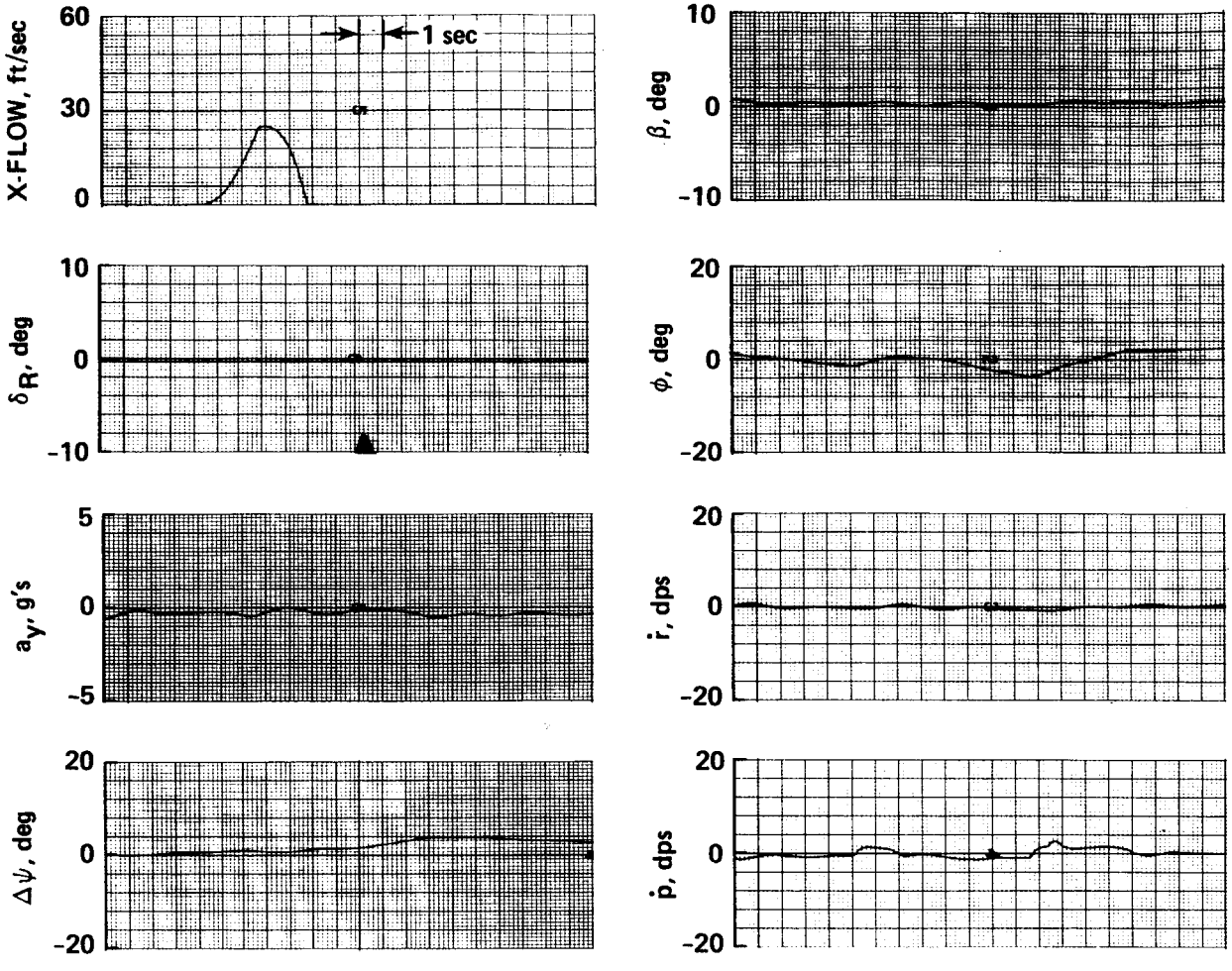

Figure 17.- Time history of entry condition 9--lateral traces.

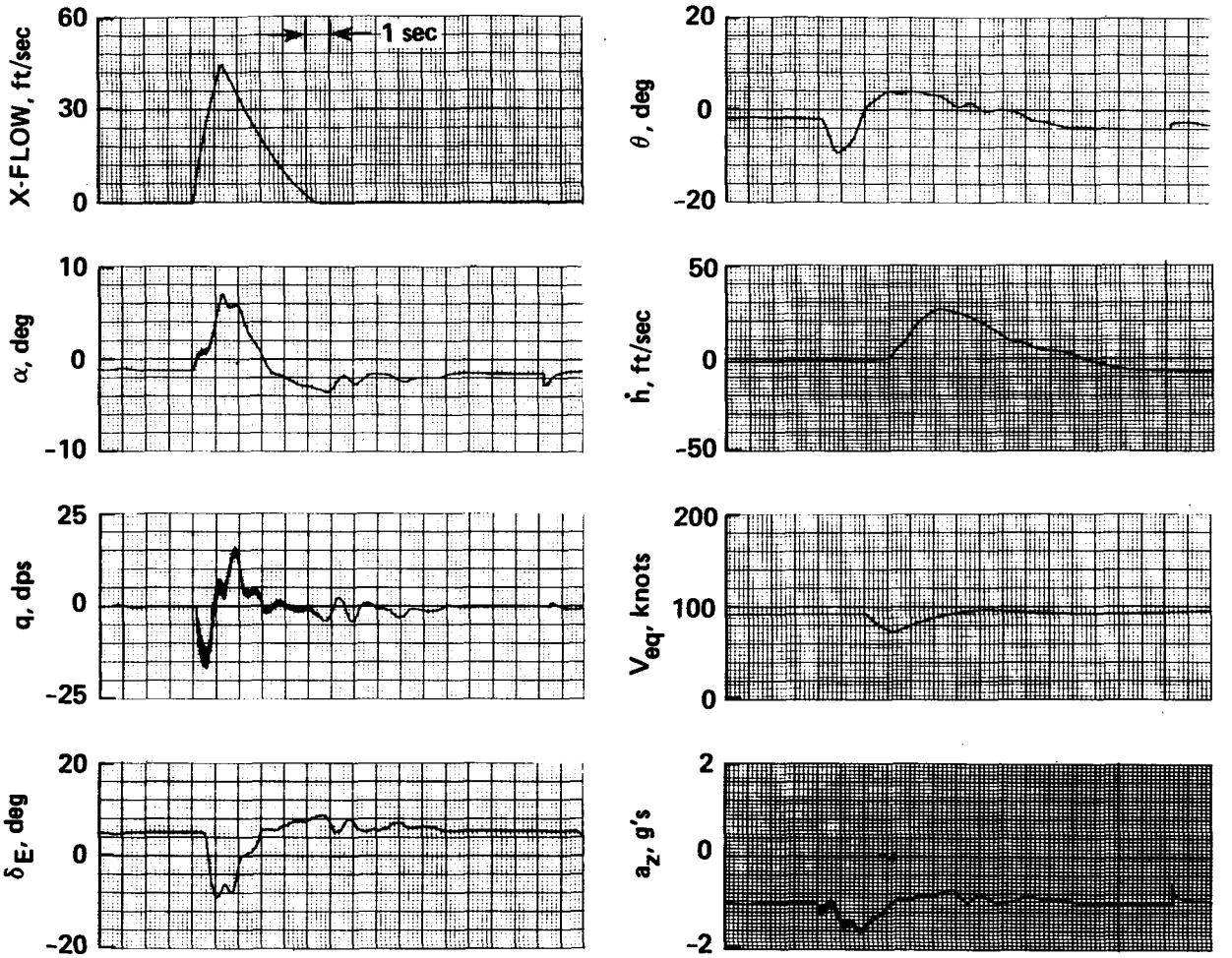

Figure 18.- Time history of entry condition 10--longitudinal traces.

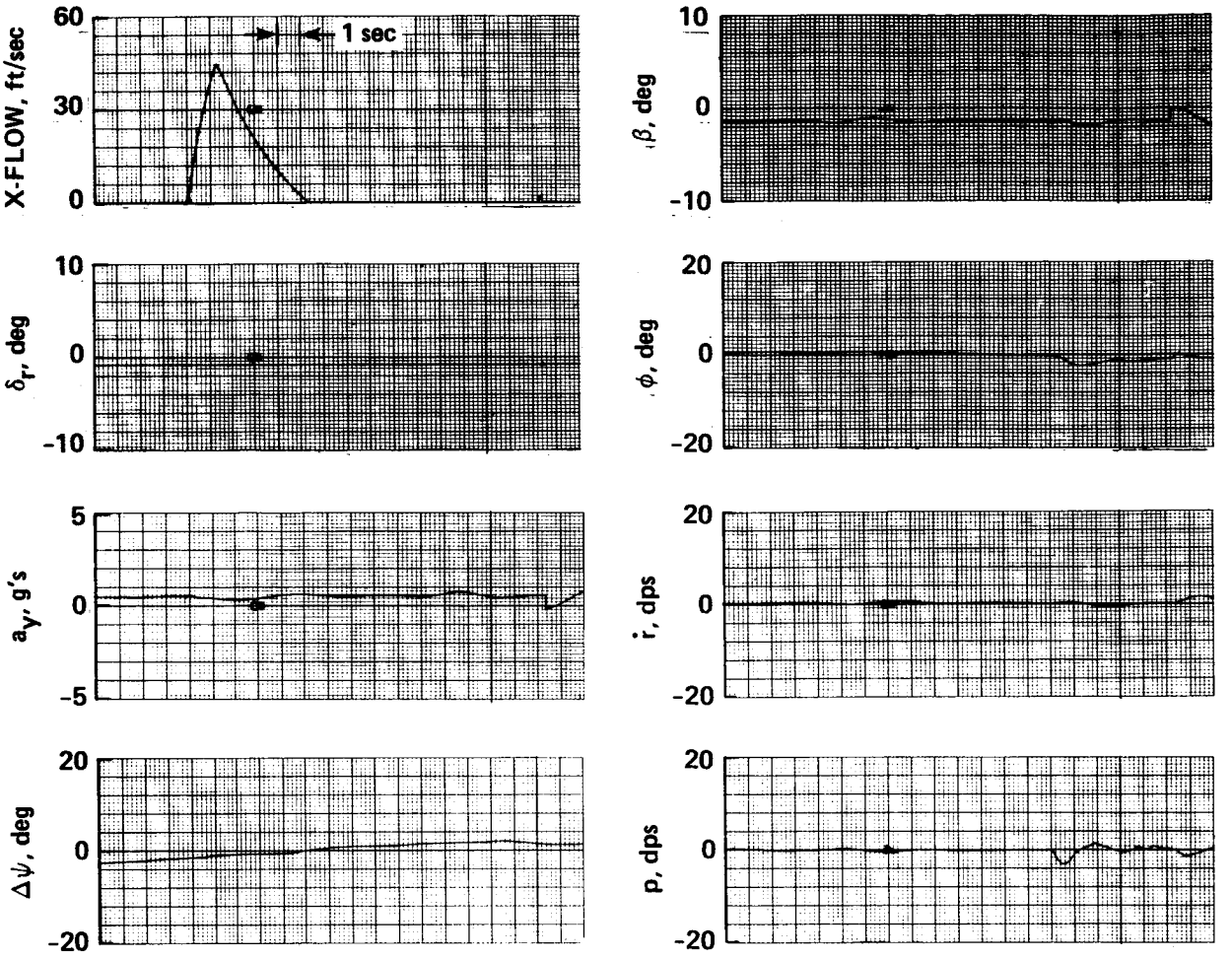

Figure 19.- Time history of entry condition 10--lateral traces.

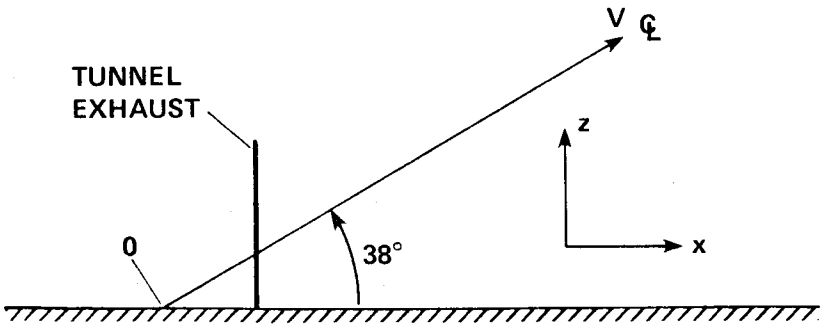

Figure 20.- Pictoral definition of virtual origin.

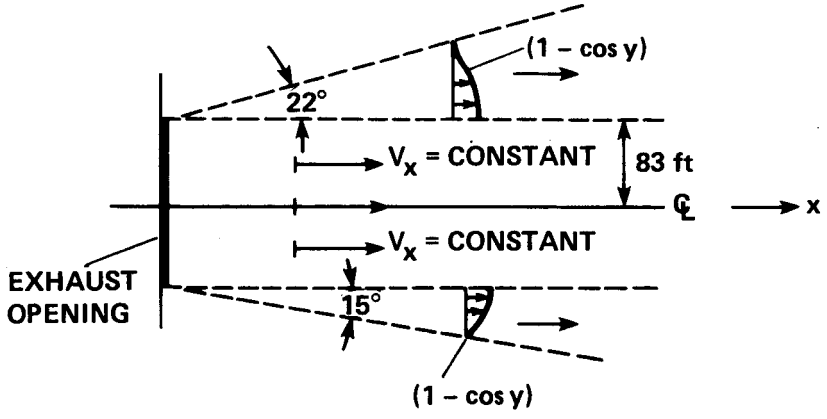

Figure 21.- Planform of the modeled exhaust flow.

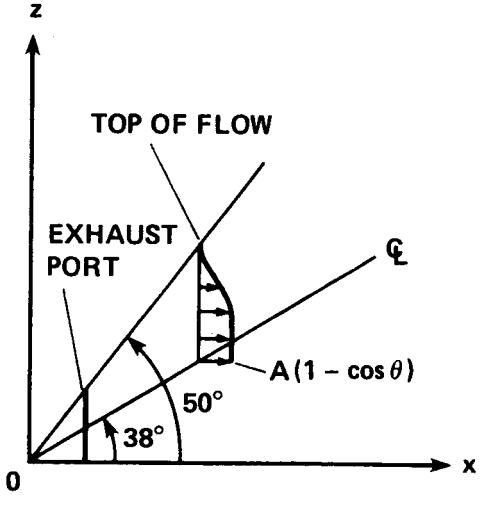

Figure 22.- Modeled flow: top.

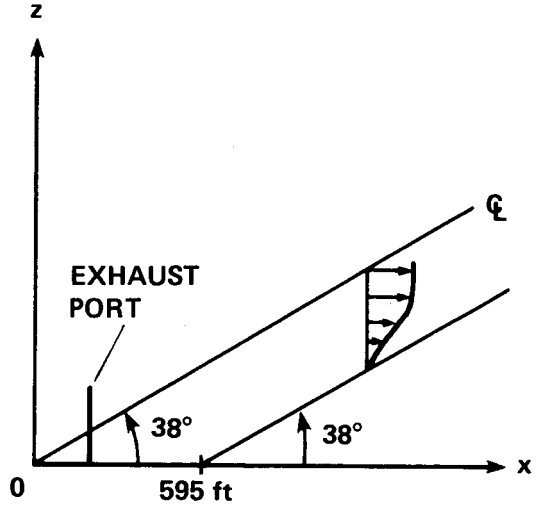

Figure 23.- Modeled flow: bottom.

```
C
C       XCG,YCG = COORDINATES OF THE AIRPLANE ON THE TERRAIN BOARD
C       XTEF0,YTEF0 = COORDINATES OF THE WIND TUNNEL ON THE BOARD
C       VEW = VECTOR COMPONENT OF WIND TO THE EAST
C       VDW = VECTOR COMPONENT OF WIND DOWNWARD
C
 1005 CONTINUE

      IF (IEXFWT .EQ. 0) GO TO 2900

      DXCGTEF = XCG - XTEF0
      DYCGTEF = YCG - YTEF0

      IF (ABS(DXCGTEF) .GT. 1841.0) WXVEL = 0.0; GO TO 2600

      DXCGE125 = DXCGTEF - 125.
      DXCGEM83 = DYCGTEF - 83.
      DXCGEP83 = DYCGTEF + 83.

      WXVEL = 64.0
      IF (DXCGTEF .LT. 0.) WXVEL = 0.0
      IF (DXCGTEF .GT. 425.) WXVEL = 64.+(DXCGTEF-425.)*(-0.0452)

      IF (DYCGTEF .LE. 83. .AND. DYCGTEF .GE. -83.) GO TO 2200

 2000 IF (DYCGTEF) 2300,2200,2100

 2100 IF ((ABS(DYCGEM83))/DXCGE125 .LE. TAN15)
     *   WXVEL = WXVEL*(1.-(ABS(DYCGEM83))/(DXCGE125*TAN15));
     *   GO TO 2200

      WXVEL = 0.0

 2300 IF (ABS(DYCGEP83)/DXCGE125 .LE. TAN22)
     *    WXVEL = WXVEL*(1.-(ABS(DYCGEP83))/(DXCGE125*TAN22));
     *    GO TO 2200

      WXVEL = 0.0

 2200 CONTINUE

      IF (WXVEL .EQ. 0.) GO TO 2600

      IF (HCG-DXCGTEF*TAN38) 2500,2600,2700

 2500 IF (HCG .LT. (DXCGTEF*TAN38-465.)) WXVEL=0.; GO TO 2600
      WXVEL = WXVEL*(1.-(ABS(DXCGTEF*TAN38-HCG))/465.)
      GO TO 2600


 2700 IF (HCG .GE. (DXCGTEF*TAN50)) WXVEL=0.; GO TO 2600
      WXVEL=WXVEL*(1.-(HCG-DXCGTEF*TAN38)/
     *                (DXCGTEF*(TAN50-TAN38)))

 2600 CONTINUE

      VEW = WXVEL
      VDW = - WXVEL * TAN38

 2900 CONTINUE

      CALL BWIND(DT3)

 9999 CONTINUE

      RETURN
      END
```

Figure 24.- FORTRAN code of the wind tunnel flow.

1. Report No. NASA TM-86819	2. Government Accession No.	3. Recipient's Catalog No.
4. Title and Subtitle SIMULATION INVESTIGATION OF THE EFFECT OF THE NASA AMES 80- BY 120-FOOT WIND TUNNEL EXHAUST FLOW ON LIGHT AIRCRAFT OPERATING IN THE MOFFETT FIELD TRAFFIC PATTERN		5. Report Date February 1986 6. Performing Organization Code
7. Author(s) Barry G. Streeter		8. Performing Organization Report No. A-85372 10. Work Unit No.
9. Performing Organization Name and Address Ames Research Center Moffett Field, CA 94035		11. Contract or Grant No. 13. Type of Report and Period Covered Technical Memorandum
12. Sponsoring Agency Name and Address National Aeronautics and Space Administration Washington, DC 20546		14. Sponsoring Agency Code 505-61-71

15. Supplementary Notes

Point of Contact: Barry G. Streeter, Ames Research Center, M/S 211-2, Moffett Field, CA 94035 (415) 694-5449 or FTS 464-5449

16. Abstract

A preliminary study of the exhaust flow from the Ames Research Center's 80- by 120-Foot Wind Tunnel indicated that the flow might pose a hazard to low-flying light aircraft operating in the Moffett Field traffic pattern. A more extensive evaluation of the potential hazard was undertaken using a fixed-base, piloted simulation of a light, twin-engine, general-aviation aircraft. The simulated aircraft was "flown" through a model of the wind tunnel exhaust by pilots of varying experience levels to develop a data base of aircraft and pilot reactions. This study shows that a light aircraft would be subjected to a severe disturbance which, depending upon entry condition and pilot reaction, could result in a low-altitude stall or cause damage to the aircraft tail structure.

17. Key Words (Suggested by Author(s))	18. Distribution Statement
General-aviation aircraft Ames 80- by 120-Foot Wind Tunnel Wind shear	Unlimited Subject category - 03

19. Security Classif. (of this report)	20. Security Classif. (of this page)	21. No. of Pages	22. Price*
Unclassified	Unclassified	32	A03

*For sale by the National Technical Information Service, Springfield, Virginia 22161